

PAPER

Tripled critical current in racetrack coils made of Bi-2212 Rutherford cables with overpressure processing and leakage control

To cite this article: Kai Zhang *et al* 2018 *Supercond. Sci. Technol.* **31** 105009

View the [article online](#) for updates and enhancements.



IOP | ebooks™

Bringing you innovative digital publishing with leading voices to create your essential collection of books in STEM research.

Start exploring the collection - download the first chapter of every title for free.

Tripled critical current in racetrack coils made of Bi-2212 Rutherford cables with overpressure processing and leakage control

Kai Zhang¹ , Hugh Higley¹, Liyang Ye¹, Steve Gourlay¹, Soren Prestemon¹, Tengming Shen¹ , Ernesto Bosque², Charles English², Jianyi Jiang², Youngjae Kim², Jun Lu² , Ulf Trociewitz², Eric Hellstrom² and David Larbalestier²

¹Lawrence Berkeley National Laboratory, Berkeley, CA 94720, United States of America

²National High Magnetic Field Laboratory, Florida State University, Tallahassee, FL 32310, United States of America

E-mail: tshen@lbl.gov

Received 10 May 2018, revised 23 July 2018

Accepted for publication 14 August 2018

Published 6 September 2018



CrossMark

Abstract

We fabricated three racetrack coils (RC1, RC2, and RC3) from Bi-2212 Rutherford cables (17-strand, thickness \times width = 1.44 mm \times 7.8 mm, strand diameter = 0.8 mm) and applied overpressure processing heat treatment (OPHT). The quench currents of RC1 and RC2 reached 5268 A and 5781 A, respectively, despite them still, surprisingly, exhibiting some Bi-2212 leakage to the surface. After removing most of the leakages using a simple-to-implement insulation scheme, the quench current of RC3 improved to 6485 A, which is about three times the average quench current of a dozen racetrack coils that had been fabricated and reacted using the conventional 1 bar heat treatment. The results confirm the effectiveness of the OPHT technology and the new leakage control scheme for coils made from Bi-2212 Rutherford cables. Coils exhibited an increased quench current with increasing the current ramp rate from 5 to 200 A s⁻¹; they were quite stable against point and transient disturbances, and were capable of adsorbing persistent Joule heating at \sim 80 mW for $>$ 15 s before quenching. These behaviors are different from Nb-Ti and Nb₃Sn accelerator magnets. Overall, our results provide a critical evaluation and verification of Bi-2212 wire and magnet technologies (wire, insulation, heat treatment, coil fabrication, and coil operation), reveal crucial new stability features of Bi-2212 magnets, and demonstrate technological options for it to become a practical high-field magnet technology.

Keywords: Bi-2212, overpressure processing, accelerator magnet, quench, HTS racetrack coil

(Some figures may appear in colour only in the online journal)

1. Introduction

Like Nb-Ti and Nb₃Sn, Bi-2212 is available as an isotropic, multifilamentary round wire and can be made into 5–20 kA Rutherford cables and 10–100 kA cable-in-conduit cables [1–3]. At 4.2 K this high- T_c cuprate round wire conductor also carries a high critical current density J_c that slowly declines

with increasing magnetic fields, and carries high J_c well above 20 T. For example, a high J_c of 950 A mm⁻² at 4.2 K and 45 T was demonstrated by Oxford Superconducting Technology (OST, now Bruker OST) in 2005 [4]. However, efforts at making superconducting coils using Bi-2212 wires for a few years after 2005 yielded disappointing results. For example, a dozen racetrack coils made from Bi-2212

Table 1. Parameters for the racetrack coils fabricated. Wires were fabricated by Bruker OST using the powder-in-tube technique. They share a similar Ag:Ag-0.2 wt%Mg:Bi-2212 ratios. The RC3 Rutherford cable was painted with a TiO₂ coating before insulated with a mullite sleeve insulation.

Coil ID	RC1	RC2	RC3
Wire ID	PMM130411	PMM120928	PMM120928
Wire design	19 × 36	37 × 18	37 × 18
Precursor powder	Nexans batch #77, composition Bi _{2.17} Sr _{1.94} Ca _{0.89} Cu _{2.00} O _x		
Filament twisted	No		
Witness round wire diameter (mm)	0.8 mm (as-drawn), ~0.775 mm (after 50 bar OPHT)		
Witness strand J_E (4.2 K, 14 T) (A mm ⁻²) after 50 bar OPHT	~420	~500	~500
LBNL cable ID	1066	1067	1067
Cable design	17-strand, 1.44 mm × 7.8 mm (bare), pitch angle = 15°, pitch length = 55 mm, packing factor = 82%		
Cable length	7.5 m		
Insulation	Braided mullite sleeve	Braided mullite sleeve	TiO ₂ + braided mullite sleeve
Mullite sleeve thickness	~150 μm		
Heat treatment	50 bar OPHT in a mixture of Ar/O ₂ ($P(O_2) = 1$ bar)		
Impregnation	Beeswax	Beeswax	NHMFL mix 61 epoxy
Field generation constant	0.4065 T kA ⁻¹		

Rutherford cables at Lawrence Berkeley National Laboratory (LBNL) using a wind-and-react approach showed a wire J_c much lower than critical current test barrel values shown by OST [5, 6]. Despite these coils being made in a meticulous manner to avoid contamination, they exhibited leakage, signs of the Bi-2212 liquid phase inside Bi-2212 filaments leaking out of the silver matrix during heat treatment and reacting with the insulation.

Further studies revealed that a basic problem of Bi-2212 wire is that it is a powder-in-tube wire in which there is necessarily porosity so as to allow the Bi-2212 powder particles to slide over one another during the wire fabrication [7–10]. At the end of wire manufacture this porosity is typically about 35%, very well distributed and generally invisible in wire cross-sections. On heating the wire into and through the partial melt state, the gas inside these pores expands about four times. If the wire ends are closed or the wire is long, these internal gases cannot escape and thus cause significant creep of the Ag, wire expansion and Bi-2212 dedensification, and even wire burst. By contrast, gas can generally escape in short wires reacted with open ends [11], thus avoiding this long length wire problem. The J_c of such wires is generally much higher than in coil-length wires. Leakage is thus a natural consequence of the internal gas pressure and the creep rupture of silver sheath that it causes, which manifests as longitudinal cracks parallel to the wire axis that relieve the principal circumferential stress in the wire sheath [12]. Overpressure processing heat treatment (OPHT) was devised to prevent this Ag creep by using an external gas pressure to counteract wire expansion. OPHT shrinks wire diameters and almost fully densifies the Bi-2212 filaments, raising the J_c in wires [13] substantially above those obtained previously by OST [4]. It was successfully applied to a solenoid wound from single round strands (10 bar OPHT), which generated an additional 2.6 T in a background field of 31.2 T for a total

field of 33.8 T [13]. More typically a 50 bar OPHT is now applied as a standard HT.

However there were still concerns towards applying the OPHT technology to practical coils, such as those required for accelerator magnets [14]. A key question was its applicability to coils made with Rutherford cables, in which strands are twisted, rolled, and heavily deformed, especially at the edges of cables. Coils useful for accelerator magnets, including racetrack coils [15], cosine-theta coils, and canted cosine-theta coils [16, 17], are all reacted inside a fixture that defines their shapes during reaction but they are made using alloys such as stainless steels and Inconel. A concern was that these materials react with oxygen and can cause local oxygen deprivation, therefore changing the reaction and Bi-2212 stoichiometry, thus reducing J_c . Bi-2212 needs diligent processing control (peak processing temperature and the time in the melt among others) [18, 19], and this control needs to be applicable, reliable, and reproducible to a relatively large thermal mass sitting in a high density, high pressure gas mixture (Ar and O₂ with a total pressure of >25 bar and with an oxygen partial pressure of 1 bar). Racetrack coils are a great tool for examining these and other issues relevant to fabrication and operation of practical accelerator magnets [20]. Here we apply the OPHT for the first time to racetrack coils made using Bi-2212 Rutherford cables.

2. Experiment design

2.1. Conductor, coil design, and coil fabrication

Table 1 lists specifications of the three two-layer, six-turn/layer racetrack coils (RC1, RC2 and RC3) fabricated for these experiments. All three coils were wound using the ‘double-pancake’ technique with each coil having two layers, each of which is comprised of six turns; the ramp turn between the

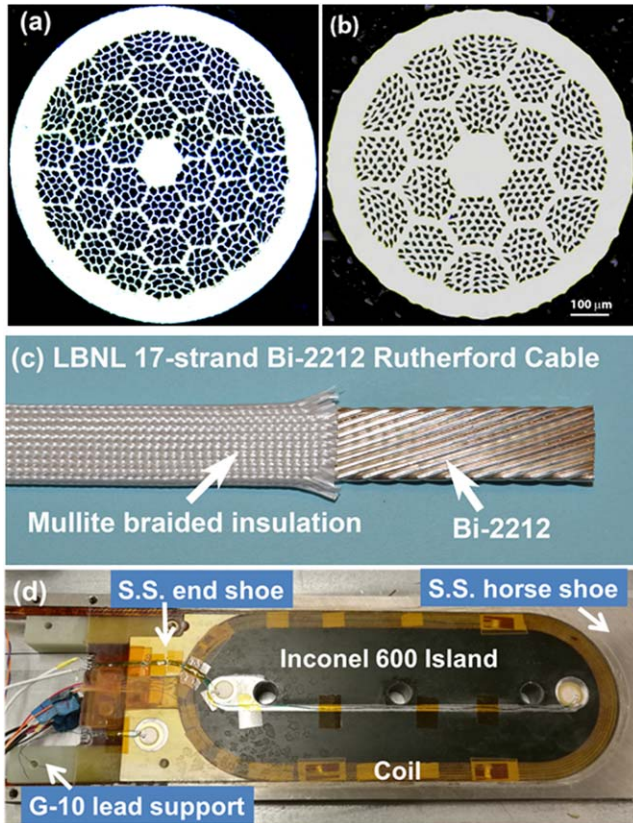


Figure 1. (a) Transverse cross-section of RC1 strand PMM130411, and (b) transverse cross-section of RC2/3 strand PMM120918. (c) An insulated 17-strand Bi-2212 Rutherford cable. (d) RC3 after potting. S.S. = stainless steel.

two layers is in the highest field region. Coils were wound on an UHV cleaned and preoxidized INCONEL[®] 600 island (straight length = 152.4 mm; arc radius = 39.4 mm). Voltage taps made of pure Ag foil were added during coil winding. After winding, the coil was enclosed inside a package of preoxidized INCONEL[®] 600 tooling consisting of a horseshoe, an end shoe, and two lead support pieces. The coil pack was then assembled inside two preoxidized Inconel[®] 600 plates and shipped to the National High Magnetic Field Laboratory (NHMFL) for OPHT. The weight of the reaction package is ~ 8.2 kg and it measures 370 mm \times 120 mm \times 31 mm.

A key difference between RC1 and RC2 is that the wire was changed from a wire with a 19 \times 36 architecture (36 bundles, each having 19 filaments) to a wire with a 37 \times 18 architecture. RC3 is identical to RC2 except that its cable was brush painted with several coats of TiO₂-polymer slurry before being insulated with the same mullite sleeve used for the cables and coil winding of RC1 and RC2. The TiO₂ slurry was prepared with a recipe [21, 22] used for single strand solenoids with properties already reported [23–25]. Figure 1 shows cross-sections of the wires and the insulated Rutherford cable. The RC2 and RC3 strand (PMM120928) represents the state-of-the-art industrial wires fabricated from 2005–2016 whereas the RC1 strand (PMM130411) has a sub-par performance.

2.2. Heat treatment and impregnation

To prepare coils for OPHT, coils were heat treated at 450 °C for 4 h in flowing O₂ ($p_{O_2} = 1$ bar) to remove the organic sizing in the braided mullite insulation sleeve [6], and the ends of their strands were sealed using hydrogen torches. After that, the coil package was vertically positioned inside the NHMFL overpressure process (OP) furnace and reacted using a peak reaction temperature of ~ 892 °C in a flowing mixture of argon and O₂ (Ar:O₂ = 49:1) with a total gas pressure of 50 bar [13].

To facilitate a possible postmortem examination of coils, RC1 and RC2 were impregnated with Beeswax. RC3, however, was impregnated with an epoxy developed for the NMR 900 MHz spectrometer magnet at the NHMFL (NHMFL ‘mix 61’). Before potting, the INCONEL[®] 600 horseshoe and the INCONEL[®] 600 end shoe were replaced with stainless steel counterparts; the INCONEL[®] 600 lead supports were replaced with G-10 counterpart. Figure 1 shows a photo of RC3 after epoxy impregnation. After potting, the coil was assembled inside side bars and cover plates made of stainless steel to prevent motions due to Lorentz forces during high-current tests.

2.3. Coil test

The coil was connected to a header with 10 kA vapor cooled current leads. The coil was connected to Cu current leads using two 7.8 mm wide Nb–Ti Rutherford cables. The typical joint resistance between Nb–Ti cables and Bi-2212 cable (soldered using Sn₆₂Pb₃₆Ag₂; splice length = 80 mm; Nb–Ti was soldered to both sides of Bi-2212.) is ~ 1 n Ω at 4.2 K.

Voltage signals for each layer were connected to a multichannel, 16 bit data acquisition system that sampled at both 10 Hz and 1 kHz. Voltage signals of half coils (a coil layer), the whole coil, and the imbalance value were also monitored by an FPGA board for quench detection. Typical quench detection voltage thresholds are 50 mV for the whole coil, 30 mV for layer 1, 30 mV for layer 2, and 50 mV for the voltage imbalance between half coils. After detecting a quench, the power supply is turned off and a dump resistor is switched into the circuit. The coil current is then forced to decay with a time constant $\tau = L/R_D$, where L refers to the coil inductance and R_D is the value of the dump resistor ($L \approx 36.3$ μ H, $R_D \approx 20$ m Ω , and $\tau \approx 1.89$ ms).

3. Results

3.1. Overall performance

Figure 2 shows that the quench current (I_q) at 4.2 K increases with increasing current ramping rate dI/dt for RC1, RC2 and RC3. I_q is defined as the maximum current reached by the power supply upon detecting a quench while increasing the current linearly. For RC2, the I_q increases from 5483 A with $dI/dt = 10$ A s⁻¹, to 5781 A with $dI/dt = 150$ A s⁻¹, respectively whereas for RC3, the I_q increases from 6255 A with $dI/dt = 5$ A s⁻¹ to 6485 A with $dI/dt = 150$ A s⁻¹,

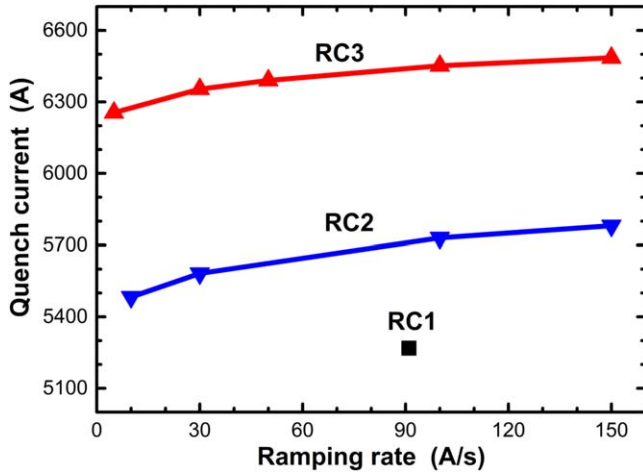


Figure 2. Dependence of I_q on the current ramping rate dI/dt for RC1, RC2, and RC3.

Table 2. Holding current tests on RC2 and RC3.

Coil	Hold current (A)	Quench?
RC1	4570	Hold for 100 s and no quench
	5085	Quench after 3.5 s
RC2	5178	Hold for 100 s and no quench
	5280	Hold for 100 s and no quench
	5380	Hold for 100 s and no quench
	5432	Quench after 20 s
	5482	Quench after 8 s
RC3	5584	Quench after 3 s
	6130	Hold for 180 s and no quench
	6200	Hold for 180 s and no quench
	6300	Quench after 5 s

respectively. This behavior is different from the well-known behavior of Nb–Ti and Nb₃Sn Rutherford cable based coils for which I_q decreases with increasing ramping rate, e.g. by $\sim 20\%$ from $dI/dt = 5 \text{ A s}^{-1}$ to $dI/dt = 150 \text{ A s}^{-1}$ for a Nb₃Sn LARP quadrupole magnet [26]. RC2 and RC3 did not exhibit the quench training found in Nb–Ti and Nb₃Sn accelerator magnets [27, 28]. Moreover, repeated tests yielded the same I_q within $\pm 5 \text{ A}$. With a field generation constant of 0.4065 T kA^{-1} , the peak field generated by RC3 is 2.64 T.

Table 2 summarizes the results of current hold tests at 4.2 K. The coils can be held in a stable manner at a current slightly below the lowest I_q determined by the linear current ramp test. For example, the lowest I_q for RC3 was 6255 A. RC3 was ramped up to 6200 A at $dI/dt = 50 \text{ A s}^{-1}$ and then could sit at 6200 A for 180 s without quenching. After a current ramp to 6300 A at 50 A s^{-1} , it quenched at 6300 A after only 5 s.

3.2. V – I characteristics at 4.2 K and quench origins

Figure 3 shows coil and turn voltages of RC2 during a linear current ramp of 10 A s^{-1} . Figure 4 shows an example of coil and turn voltages of RC2 during a current hold test at 5432 A at 4.2 K that results in a thermal run-away and a current dump

after 20 s. Both cases result in a quench with characteristics of V_{Layer1} and V_{ete} increasing positively, driven by increasing internal resistance, and V_{Layer2} going negative, driven by inductive voltages. When V_{ete} reached 0.1 V at $t = 55.839 \text{ s}$ (figure 3), voltages of several turns (L1-T5, LT-T6, ramp turn, L2-T6, and L2-T5) had turned positive, showing resistive transitions at these turns and that the quench was not pointlike in nature; similarly, when V_{ete} reached 0.1 V at $t = 63.700 \text{ s}$ (figure 4), voltages of the inner turns (L1-T5, LT-T6, ramp turn, L2-T6, and L2-T5) had turned positive. When RC2 was held at a constant current before the quenches (figure 4), the quenching turns also showed higher resistive voltages at $t = 50 \text{ s}$ ($I = 5432 \text{ A}$) than at $t = 35 \text{ s}$ ($I = 5075 \text{ A}$) (for example, the voltage of the ramp turn increased from 1.3 to $11 \mu\text{V}$), due to increasing index losses when increasing superconductor current around its critical current.

3.3. Bi-2212 leakage

Overpressure processing had been expected to prevent the creep rupture of silver [12], therefore eliminating leakages. Surprisingly, leakage was still observed on RC1 and RC2 (figure 5). Most leakage was present at cable edges. Painting the Rutherford cable with a TiO₂ slurry before insulating it with the mullite sleeve nearly removed all leakage spots after 50 bar OPHT. As shown in figure 6, only six leakage spots were visible for the layer 1 of RC3. As noted also in some solenoid coils at the NHMFL, it appears that there can be a thermodynamically-driven leakage mechanism during the highest temperature portion of the heat treatment in which constituents of the Bi-2212 core can diffuse through the Ag to react with metallic oxide formers. TiO₂ is an effective barrier to such diffusion here and in the solenoids.

3.4. Conductor cross-sections

Figure 7 shows an optical micrograph of the transverse cross-section of a piece of Ag/Bi-2212 cable from RC1 that contains leakage. The strand at the edge of the cable lost a portion of its filaments. Interesting no silver ruptures (‘open wounds’) like those observed by Shen *et al* [12] were observed, despite careful and gradual sectioning. For a round strand, the 50 bar OPHT shrinks the wire diameter by $\sim 4\%$ [29]. Strands within a cable sintered together, without developing gaps between strands, while shrinking in size. The cable shrank to approximately $1.33 \text{ mm} \times 7.3 \text{ mm}$ after the OPHT. Many strands within the cable developed a peanut shape.

3.5. Performance of extracted strand tests

Strands were extracted from unreacted Rutherford cables and reacted using 50 bar OPHT, and their I_c were measured and shown in figure 8. No definitive I_c differences were found between the kinked and the straight sections.

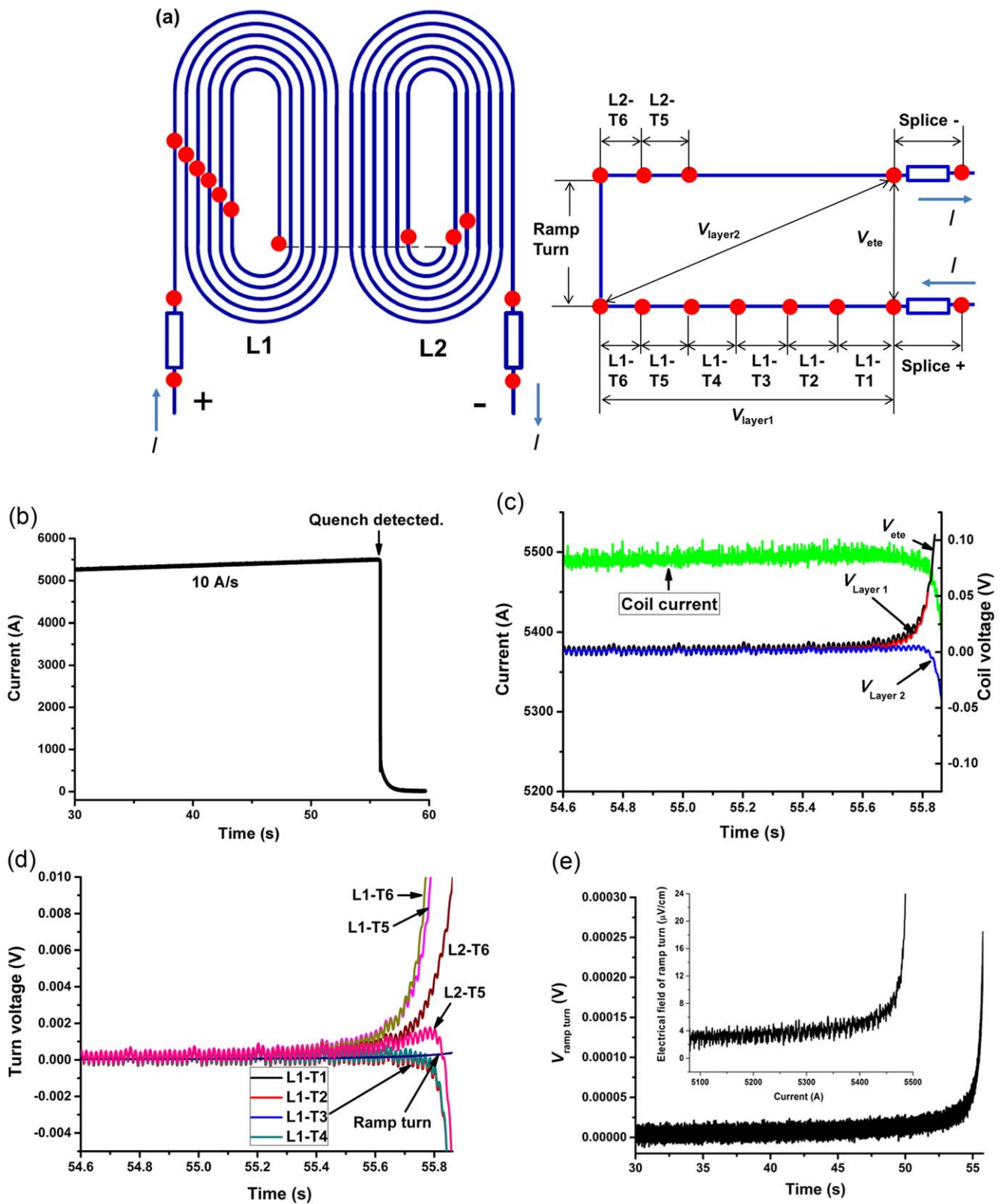


Figure 3. RC2 voltage development during a current ramping test ($dI/dt = 10 \text{ A s}^{-1}$). (a) Voltage tap connection schematics. As an example, L1-T1 means the turn 1 (the outermost turn) of the layer 1. The right hand side shows $V_{ete}(t)$, $V_{Layer 1}(t)$, and $V_{Layer 2}(t)$. (b) $I(t)$. (c) Turn voltages. (d) $V(t)$ of the ramp turn. The ramp turn is $\sim 12.3 \text{ cm}$ long. (e) $E(t)$ of the ramp turn. The inset is the $E-I$ of the ramp turn.

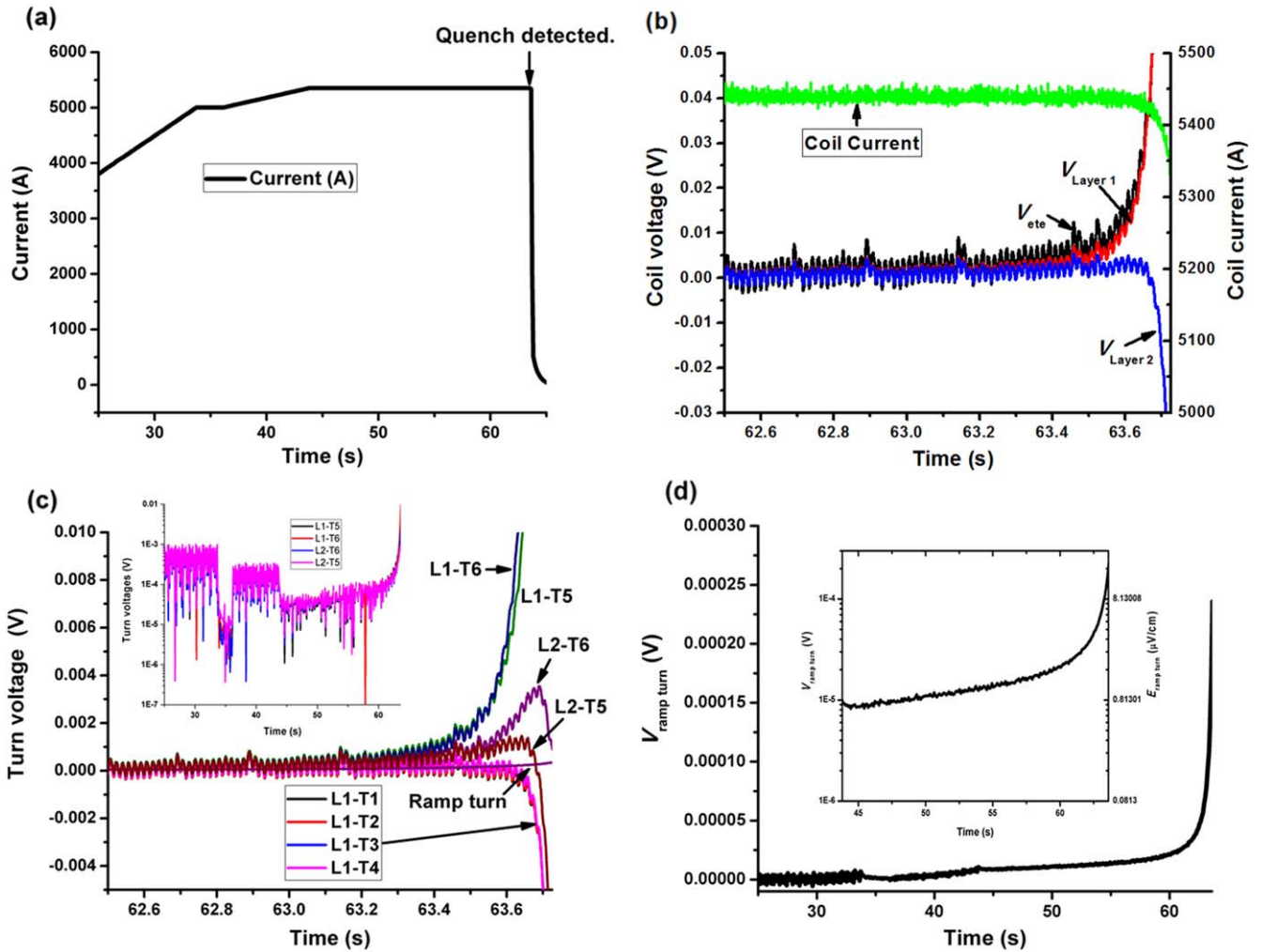


Figure 4. RC2 voltage development during a current dwelling test, during which a quench was detected and current was forced to go to zero after the magnet current was held at 5432 A for 20 s (a) $I(t)$. (b) $V_{ete}(t)$, $V_{Layer 1}(t)$, and $V_{Layer 2}(t)$. (c) Turn voltages. (d) The ramp turn voltage.

4. Discussion

4.1. Bi-2212 racetrack coil technology: reaching a new height with OPHT

Figure 9 compares the quench current of RC1, RC2, and RC3 with previous coils fabricated at LBNL using the conventional 1 bar heat treatment. The critical currents I_c (determined with the electrical field criterion $E_c = 10^{-5} \text{ V m}^{-1}$) of previous coils at 4.2 K, self-field are 1526 A for HTS-SC-04, 1711 A for HTS-SC-06, 2636 A (quench value) for HTS-SC-08 and 2417 A for HTS-SC-10, respectively [6, 30], with an average current of 2072 A. RC3 reached 6485 A, more than tripling this benchmark performance. Overall, all three RC coils show good performance, providing a first proof that the OPHT Bi-2212 coils can be reliable and reproducible (at least for the coil sizes of RC1–3).

Figure 10 compares the $J_E(B)$ characteristic of the strand PMM120928 used for RC2 and RC3 after 1 bar HT and 50 bar OPHT to that of the strand PMM 070420 used for HTS-SC08 after 1 bar HT, together with the load lines of the HTS-SC and RC coils. HTS-SC-08 reached $\sim 80\%$ of its short

sample limit whereas RC1, RC2 and RC3 reached $\sim 91\%$, $\sim 88\%$ and $\sim 97\%$ of their respective short sample limits along the load line. Figure 10 also shows that the performance improvement of the HTS-SC coils to RC1 and RC2 are mostly due to the large benefits to J_c of the OPHT. Using 1 bar HT samples wound from 1 m long wires reacted with their ends open on ITER barrels, we found that J_E of the 1 bar HT strand PMM120928 (320 A mm^{-2} at 4.2 K and 5 T) was only slightly better than that of the strand PMM 070420 (270 A mm^{-2}). By contrast the 50 bar HT raised J_E of the single strand to 674 A mm^{-2} at 4.2 K and 5 T. The further J_E improvement from RC2 to RC3 is likely due to the reduced leakage resulting from the added TiO_2 layer.

4.2. Leakage mechanisms and an insulation scheme for leakage control

Leakage has long been a problem for Bi-2212 coils [31], although the NHMFL solenoids mostly found no leakage after OP reaction. When we did see leakage we observed that there was always a continuous diffusion path between the Bi-2212 and a highly stable metal oxide of the sort found in

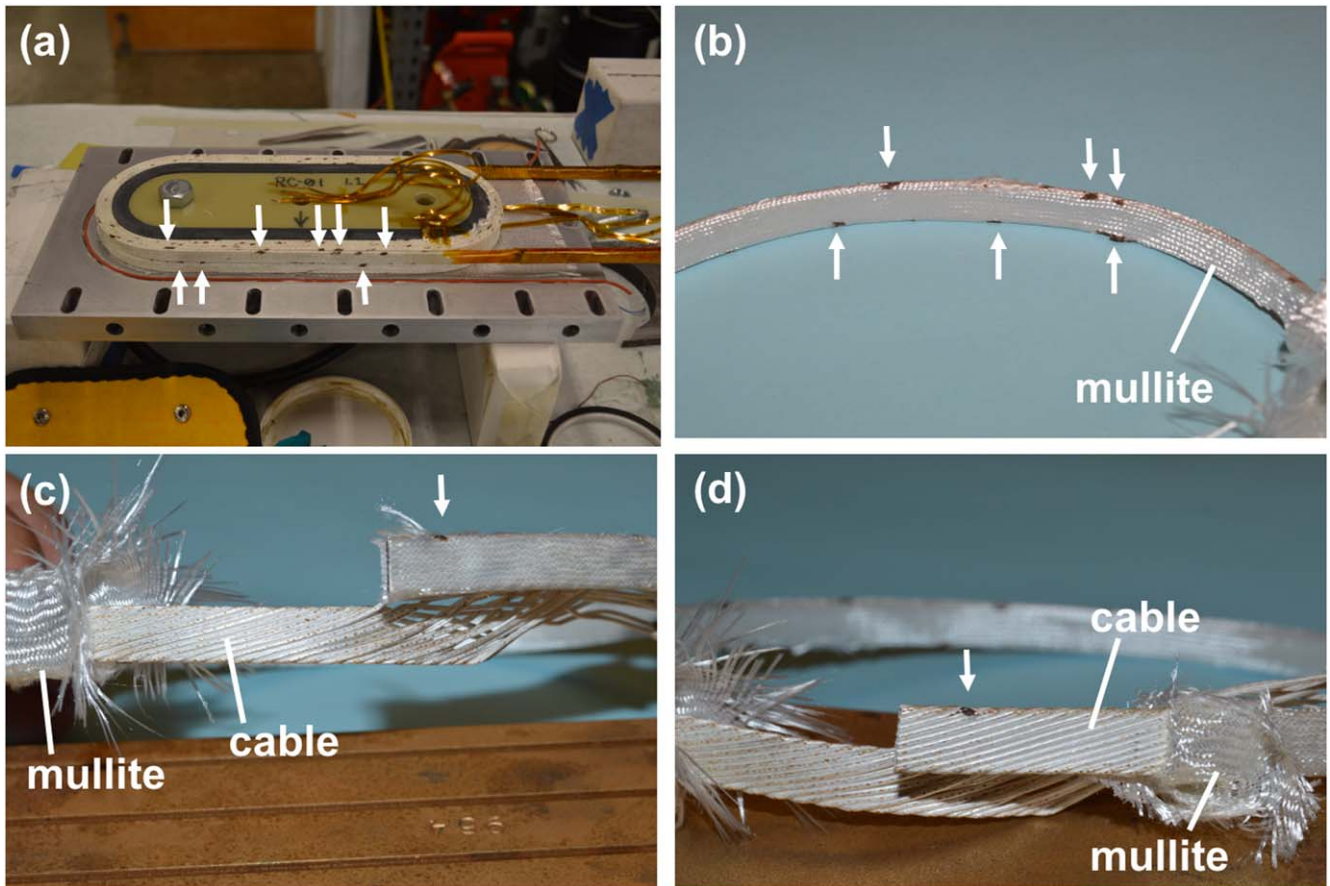


Figure 5. Typical leakage pattern in RC1 and RC2. (a) RC1 after reaction. (b) Most leakage (black areas) appears at the cable edge. A leakage spot before (c) and after (d) the mullite insulation sleeve was removed.

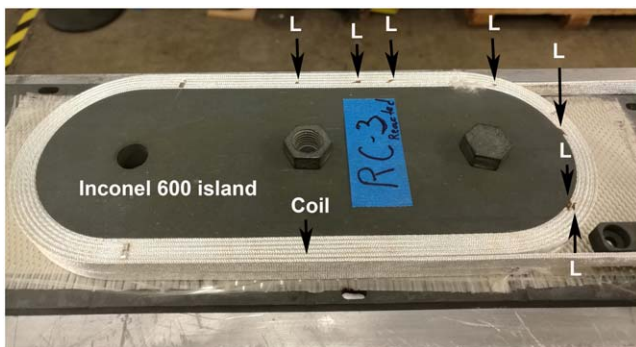


Figure 6. RC3 after reaction with its layer 1 exhibiting only seven leakage spots. L = Leakage.

Inconel. We postulated that this allowed a second mechanism of leakage unconnected to the creep rupture of the Ag generated by internal gas pressure. We call this a thermodynamic leakage mechanism that is possible because essentially any element that can dissolve in Ag at the reaction temperature is then capable of diffusing to a lower energy reaction state. The surprising leakage in RC1 and RC2 is consistent with this mechanism. The specifics here are reactions between the Ag/Bi-2212 wire and the mullite insulation that draw Bi-2212 towards the Inconel 600 reaction box [32]. Insulating Bi-2212 wires with TiO₂ plus mullite sleeve insulation seems

to effectively remove such reactions and therefore leakage, as demonstrated by solenoids earlier and again in RC3. The key in either case is to interpose an impermeable barrier between the wire and the reaction box for which TiO₂ is a simple and effective solution.

4.3. Coil stability and quench origins

Nb–Ti and Nb₃Sn magnets rarely reach their short sample J_c . They are generally unstable and show premature quenches triggered by localized, transient, and fast disturbances such as flux jump, epoxy cracking, and conductor motion. Their instability has been well documented and clearly implied by the sharp decrease of their J_c with temperature and magnetic field. It is reflected also a decrease in their quench current with increasing ramp rate due to conductor heating induced by increasing AC losses. Here the inverse ramp rate dependence of I_q in RC1, RC2, and RC3 and the absence of quench training are important evidence of a significantly higher stability of Bi-2212 magnets, which is not surprising given the slow decline of its J_c with increasing temperature and magnetic field. At 2.5 T, the T_c of Bi-2212 wires is ~ 30 K, considerably higher than the equivalent values for Nb–Ti and Nb₃Sn.

Figures 3 and 4 show that the RC coils quench when their inner turns reach their I_c values. Their quenches are thermal

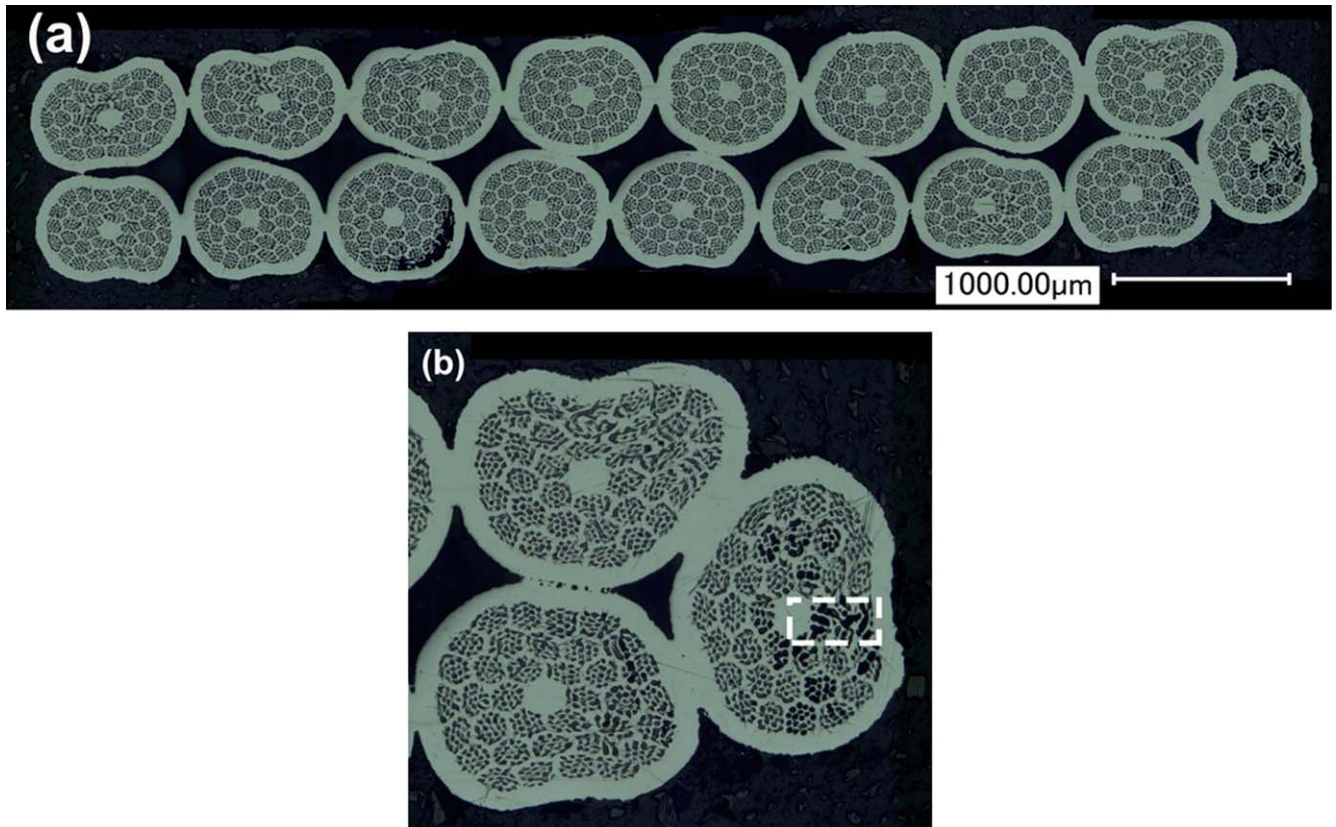


Figure 7. (a) A transverse cross-section of a RC1 cable piece that contains a leakage. (b) A magnified view of the three filaments at the right edge. The filament at the cable edge showed missing filaments, a sign of leakages, for at least the filament bundles inside the rectangle box.

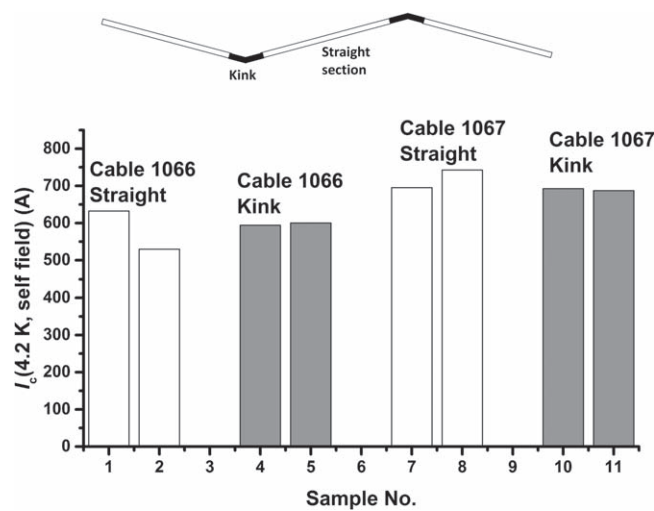


Figure 8. I_c of strands extracted from RC1 and RC2/3 Rutherford cables and reacted using the 50 bar OPHT.

run-away events driven by Joule heating coming from the slight resistance that develops as they approach their critical current. For example, for the current holding test shown in the figure 4, the resistive voltage of the ramp turn increased from $\sim 10 \mu\text{V}$ at $t = 43.7 \text{ s}$ to $\sim 20 \mu\text{V}$ at $t = 60 \text{ s}$, thus generating a steady heat input to the conductor averaging $\sim 80 \text{ mW}$ for a total heat input of $\sim 1.3 \text{ J}$ before the thermal run-away occurs at $t \approx 62 \text{ s}$. Both the amount of time that leads to this quench

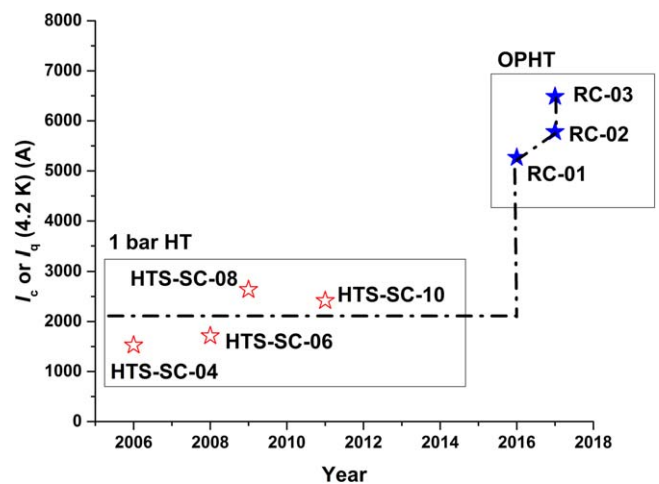


Figure 9 : Progress of I_c in LBNL Bi-2212 racetrack coils.

and the amount of energy are considerably larger than those in Nb–Ti and Nb₃Sn magnets.

5. Conclusions

In summary, three racetrack coils have been fabricated with Bi-2212 Rutherford cables and reacted with a new 50 bar OPHT and they show exceptional performance, tripling the critical current of coils made using the conventional 1 bar heat treatments. The results confirm the effectiveness of the OPHT

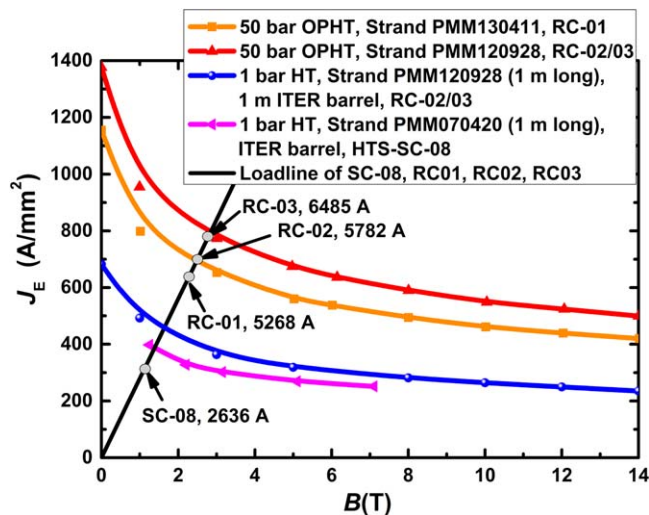


Figure 10. $J_E(B)$ of witness strands for coils RC1, RC2, RC3, and HTS-SC-08. J_E is defined as I_c/A , where the change of conductor area A is ignored and A is set to 0.5024 mm^2 . Samples for RC1, RC2, and RC3 were strands extracted from Rutherford cables and then received a 50 bar OPHT.

technology and provide a critical evaluation and verification of the Bi-2212 wire and magnet technologies (wire, insulation, heat treatment, coil fabrication, and coil operation). In addition, the work demonstrates crucial features of Bi-2212 magnets, including cable dimension changes, leakage, ramp rate dependence, and quench behavior. A new technology option of insulating cable with TiO_2 and then mullite sleeve is shown to be effective for removing leakage in RC coils.

Acknowledgments

The work at LBNL was funded by the Office of High Energy Physics (OHEP) of the US Department of Energy (DOE) through a US DOE Early Career Award. Work at LBNL was also supported by the Director, Office of Science of the US DOE under Contract No. DE-AC02-05CH11231. Kai was partially supported by a fellowship from the China Scholarship Council. Work at the NHMFL was supported by the US DOE OHEP under grant number DE-SC0010421, and by the National Science Foundation under DMR-1157490, and by the State of Florida. The authors want to thank Daniel Dietderich, Laura Garcia Fajardo, Josh Herrera, Andy Lin, Maxim Marchevsky, Emmanuele Ravaioli, Jim Swanson, Jordan Taylor, Marcos Turqueti, Xiaorong Wang, and Shijian Yin from LBNL, and George Miller from the NHMFL for technical assistance. We are all grateful to our colleagues at Bruker OST for their Bi-2212 conductors whose excellent long-length performance enables coils like this.

ORCID iDs

Kai Zhang <https://orcid.org/0000-0002-3830-9682>
 Tengming Shen <https://orcid.org/0000-0003-1581-320X>
 Jun Lu <https://orcid.org/0000-0001-8521-489X>

References

- [1] Shen T *et al* 2015 High strength kiloampere $\text{Bi}_2\text{Sr}_2\text{CaCu}_2\text{O}_x$ cables for high-field magnet applications *Supercond. Sci. Technol.* **28** 065002
- [2] Qin J *et al* 2017 Manufacture and test of Bi-2212 cable-in-conduit conductor *IEEE Trans. Appl. Supercond.* **27** 4801205
- [3] Qin J *et al* 2018 First AC loss test and analysis of a Bi2212 cable-in-conduit conductor for fusion application *Supercond. Sci. Technol.* **31** 015010
- [4] Miao H *et al* 2005 Development of round multifilament Bi-2212/Ag wires for high field magnet applications *IEEE Trans. Appl. Supercond.* **15** 2554-7
- [5] Godeke A *et al* 2009 Progress in wind-and-react Bi-2212 accelerator magnet technology *IEEE Trans. Appl. Supercond.* **19** 2228-31
- [6] Godeke A *et al* 2012 Heat treatment optimizations for wind-and-react Bi-2212 racetrack coils *Phys. Proc.* **36** 812-7
- [7] Shen T *et al* 2010 Filament to filament bridging and its influence on developing high critical current density in multifilamentary $\text{Bi}_2\text{Sr}_2\text{CaCu}_2\text{O}_x$ round wires *Supercond. Sci. Technol.* **23** 025009
- [8] Kametani F *et al* 2011 Bubble formation within filaments of melt-processed Bi2212 wires and its strongly negative effect on the critical current density *Supercond. Sci. Technol.* **24** 075009
- [9] Jiang J, Starch W, Hannion M, Kametani F, Trociewitz U, Hellstrom E and Larbalestier D 2011 Doubled critical current density in Bi-2212 round wires by reduction of the residual bubble density *Supercond. Sci. Technol.* **24** 082001
- [10] Scheuerlein C, Di Michiel M, Scheel M, Jiang J, Kametani F, Malagoli A, Hellstrom E and Larbalestier D 2011 Void and phase evolution during the processing of Bi-2212 superconducting wires monitored by combined fast synchrotron micro-tomography and x-ray diffraction *Supercond. Sci. Technol.* **24** 115004
- [11] Malagoli A, Lee P, Ghosh A, Scheuerlein C, Di Michiel M, Jiang J, Trociewitz U, Hellstrom E and Larbalestier D 2013 Evidence for length-dependent wire expansion, filament dedensification and consequent degradation of critical current density in Ag-alloy sheathed Bi-2212 wires *Supercond. Sci. Technol.* **26** 055018
- [12] Shen T, Ghosh A, Cooley L and Jiang J 2013 Role of internal gases and creep of Ag in controlling the critical current density of Ag-sheathed $\text{Bi}_2\text{Sr}_2\text{CaCu}_2\text{O}_x$ wires *J. Appl. Phys.* **113** 213901
- [13] Larbalestier D *et al* 2014 Isotropic round-wire multifilament cuprate superconductor for generation of magnetic fields above 30 T *Nat. Mater.* **13** 375
- [14] Gourlay S, Zlobin A, Prestemon S, Larbalestier D and Cooley L 2016 *The US Magnet Development Program Plan* (US Department of Energy) <https://science.energy.gov/-/media/hep/pdf/Reports/MagnetDevelopmentProgramPlan.pdf>
- [15] Zhang K *et al* 2018 3D mechanical design and stress analysis of 20 T common-coil dipole magnet for SppC *IEEE Trans. Appl. Supercond.* **28** 4004105
- [16] Godeke A *et al* 2015 Bi-2212 canted-cosine-theta coils for high-field accelerator magnets *IEEE Trans. Appl. Supercond.* **25** 4002404
- [17] Fajardo L G *et al* 2018 Designs and prospects of Bi-2212 canted-cosine-theta magnets to increase the magnetic field of accelerator dipoles beyond 15 T *IEEE Trans. Appl. Supercond.* **28** 4008305
- [18] Shen T *et al* 2011 Heat treatment control of Ag-Bi $_2$ Sr $_2$ CaCu $_2$ O $_x$ multifilamentary round wire: investigation of time in the melt *Supercond. Sci. Technol.* **24** 115009
- [19] Shen T, Li P and Ye L 2018 Heat treatment control of Bi-2212 coils: I. Unravelling the complex dependence of the critical

- current density of Bi-2212 wires on heat treatment *Cryogenics* **89** 95–101
- [20] Gourlay S A *et al* 2000 Design and fabrication of a 14 T, Nb₃Sn superconducting racetrack dipole magnet *IEEE Trans. Appl. Supercond.* **10** 294–7
- [21] Kandel H *et al* 2015 Development of TiO₂ electrical insulation coating on Ag-alloy sheathed Bi₂Sr₂CaCu₂O_{8-x} round-wire *Supercond. Sci. Technol.* **28** 035010
- [22] Lu J *et al* 2016 Ceramic insulation of Bi₂Sr₂CaCu₂O_{8-x} round wire for high-field magnet applications *IEEE Trans. Appl. Supercond.* **26** 7701005
- [23] Chen P *et al* 2013 Performance of titanium oxide–polymer insulation in superconducting coils made of Bi-2212/Ag-alloy round wire *Supercond. Sci. Technol.* **26** 075009
- [24] Chen P *et al* 2017 Experimental study of potential heat treatment issues of large Bi-2212 coils *IEEE Trans. Appl. Supercond.* **27** 4601405
- [25] Hossain *et al* 2017 Effect of sheath material and reaction overpressure on Ag protrusions into the TiO₂ insulation coating of Bi-2212 round wire *IOP Conf. Ser.: Mater. Sci. Eng.* **279** 012021
- [26] Ambrosio G *et al* 2011 Test results of the first 3.7 m long Nb₃Sn quadrupole by LARP and future plans *IEEE Trans. Appl. Supercond.* **21** 1858–62
- [27] Lietzke A F *et al* 2004 Test results for HD1, a 16 Tesla Nb₃Sn dipole magnet *IEEE Trans. Appl. Supercond.* **14** 345–8
- [28] Bajas H *et al* 2013 Cold test results of the LARP HQ Nb₃Sn quadrupole magnet at 1.9 K *IEEE Trans. Appl. Supercond.* **23** 4002606
- [29] Matras M R *et al* 2016 Understanding the densification process of Bi₂Sr₂CaCu₂O_x round wires with overpressure processing and its effect on critical current density *Supercond. Sci. Technol.* **29** 105005
- [30] Godeke A *et al* 2010 wind-and-react Bi-2212 coil development for accelerator magnets *Supercond. Sci. Technol.* **23** 034022
- [31] Schwartz J *et al* 2008 High field superconducting solenoids via high temperature superconductors *IEEE Trans. Appl. Supercond.* **18** 70–81
- [32] Wesolowski D, Rikel M, Jiang J, Arzac S and Hellstrom E 2005 Reactions between oxides and Ag-sheathed Bi₂Sr₂CaCu₂O_x conductors *Supercond. Sci. Technol.* **18** 934